PHYSICAL REVIEW B **82**, 220404(R) (2010)

Half-metallicity in the ferrimagnet $Nb(TCNE)_2$ from first principles

Giulia C. De Fusco,[1] Barbara Montanari,[2,*] and Nicholas M. Harrison[1,3]
[1]*Department of Chemistry-Thomas Young Centre, Imperial College London, South Kensington Campus, London SW7 2AZ, United Kingdom*
[2]*STFC Rutherford Appleton Laboratory, Chilton, Didcot, Oxfordshire OX11 0QX, United Kingdom*
[3]*STFC Daresbury Laboratory, Daresbury, Warrington WA4 4AD, United Kingdom*
(Received 24 July 2010; published 15 December 2010)

Hybrid density-functional calculations performed on the metal-organic compound $Nb(TCNE)_2$ (TCNE=tetracyanoethylene) confirm it to be a ferrimagnet with a high ordering temperature for a material of its class. Most interestingly, inspection of the electronic band structure reveals that the material is a half-metal. The structure investigated is formed by layers of Nb^{2+} ions and TCNE molecules, which are bridged by additional TCNE ligands. A delicate balance between strong on-site electron correlation characteristic of the electronic *d* states in Nb^{2+} and off-site hybridization with the TCNE molecules in the layers produces a half-metallic state. These spin-polarized Nb^{2+}-$[TCNE]^{\cdot-}$ layers are then coupled ferrimagnetically with the TCNE ligands above and below. The coexistence of intrinsic high-temperature ferrimagnetism and half-metallicity in a metal-organic compound is very relevant for the emerging area of half-metallic and organic spintronics.

DOI: 10.1103/PhysRevB.82.220404 PACS number(s): 75.50.Xx, 71.15.Mb, 72.25.−b, 85.75.−d

Metal-organic magnets have been researched extensively over the last few decades because they offer the prospect of realizing magnets fabricated through controlled, low-temperature solution-based chemistry, as opposed to high-temperature metallurgical routes. In addition, in these materials magnetic properties can be tuned through synthesis. Unfortunately many of the compounds that have been synthesized and tested display magnetic order only at very low temperatures. The most prominent exception is $V(TCNE)_2$ (TCNE=tetracyanoethylene), which to date has the highest magnetic ordering temperature recorded ($T_C \approx 400$ K) for a material of this class.[1–3] Due to the paucity of structural data for this system, theoretical studies have played an important role in understanding the relationship between its magnetic, electronic, and structural properties.[4] Unfortunately, the extreme air sensitivity of this material is hampering its practical exploitation.

Attempts to advance the state of the art in the field of metal-organic compounds have been fuelled recently by the emerging area of spintronics, where the exploitation of the electronic spin, in addition to the charge, has the potential to increase processing speeds, storage densities, and to lower power consumption compared to conventional electronics.[5] The use of organic-based magnets in the area of spintronics is potentially revolutionary because organic materials can preserve the spin information over extremely long times due to their inherently weak spin-orbit coupling.[6,7] Many challenges need to be addressed, however, in the emerging field of organic spintronics.[8] One crucial issue is the injection of spin-polarized current and half-metallic materials are obvious candidates for achieving this. These materials support spin-polarized current only because a semiconducting or insulating gap is present for electrons with one spin orientation but is absent for those with the opposite spin orientation. Half-metallicity has been observed in inorganic materials such as manganese perovskites and Heusler alloys,[9–11] and in metal-DNA complexes.[12] The search for an organic half-metal has been, however, largely overlooked. Recently, two organic systems based on graphene ribbons have been predicted to develop half-metallicity when immersed in an electric field[13] or chemically modified.[14]

In this Rapid Communication, we are interested in the electronic and magnetic properties of the metal-organic compound $Nb(TCNE)_2$, closely related to the high-temperature metal-organic compound $V(TCNE)_2$. Magnetization measurements on $Nb(TCNE)_2$ thin films grown by chemical vapor deposition on Si substrates have detected thermally stable ferrimagnetic order up to 210 K, a saturation magnetization of 6×10^{-4} emu Oe g^{-1} and a coercive field of 200 Oe at 2 K.[15–17] The *first-principles* electronic-structure calculations reported here agree with experiment in finding thermally stable ferrimagnetic order. The most notable result is the intrinsic half-metallicity clearly evidenced by the inspection of the electronic band structure. While the half-metallic character emerges from the Nb-$[TCNE]^{\cdot-}$ flat layers, strong ferrimagnetic interactions occur in the Nb-$[TCNE]^{\cdot-}$ chains perpendicular to the layers. From the analysis of the electronic states it emerges that the rare combination of high-temperature ferrimagnetism and half-metallicity in this material is due to a subtle balance between the strong on-site electron correlation of the Nb^{2+} *d* states and strong off-site hybridization with the TCNE molecules. These results indicate that metal-organic compounds may be an important area of exploration for half-metallic and organic spintronics.

The structure adopted for this hybrid-exchange density-functional theory study is based on that recently proposed for the V analog[4] because the experimental determination of the structure of the Nb compound has not yet been achieved. This is a reasonable hypothesis as Nb and V belong to the same group of the periodic table, have a similar electronegativity and are expected to adopt the same (2+) oxidation state.[16,18] The crystal, displayed in Fig. 1, consists of bidimensional layers containing Nb ions fourfold coordinated to equatorial μ_4-$[TCNE]^{\cdot-}$ ligands and twofold coordinated to *trans*-μ-$[TCNE]^{\cdot-}$ apical ligands which link the layers. The resulting Nb-N coordination is sixfold. Unconstrained opti-

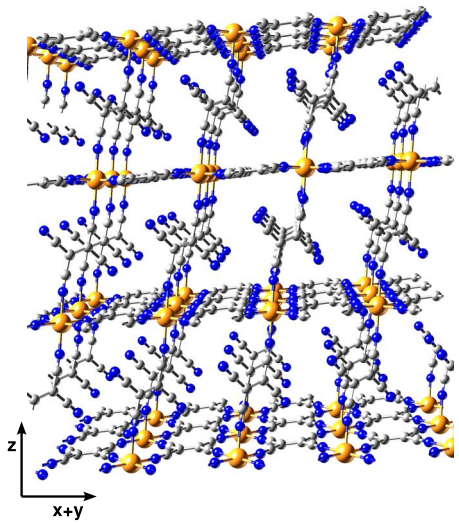

FIG. 1. (Color online) Schematic ball-and-stick representation of the unit cell of the three-dimensional $Nb(TCNE)_2$ crystal. The Nb atoms are shown in gray (gold online), the C atoms in white (gray online), and the N atoms in black (blue online). The structure consists of layers in which the Nb atoms are fourfold coordinated to $[TCNE]^-$ molecules, named *equatorial*. The layers are linked via additional $[TCNE]^-$ molecules, named *apical*. The reference frame in the bottom-left corner indicates the relationship between the atomic structure and the crystal unit cell. The lattice parameter **c** is parallel to the z direction and therefore perpendicular to the flat layers. The **a** and **b** lattice parameters are parallel to the flat layers and have similar lengths. They therefore lie at an angle of ≈45° to the $x+y$ direction.

mization of the structure results in a triclinic cell defined by a=7.39 Å, b=7.28 Å, c=10.14 Å, α=106.3°, β=97.8°, and γ=90.1°. The calculations have been performed using the hybrid-exchange density-functional B3LYP (Refs. 19–21) as implemented in the CRYSTAL06 software package.[22] The crystalline orbitals are expanded as a linear combination of atom-centered Gaussian-type functions (linear combination of atomic orbitals). The Nb basis set is a 976-31d631G contraction. The second period elements (C and N) are described with 6-31G(d) contraction double valence basis sets. A Monkhorst-Pack grid of shrinking factor equal to 6 (112 k points in the irreducible Brillouin zone) is used after finding it to be sufficient to converge the total energy to within 10^{-3} eV per unit cell (p.u.c.). The truncation of the Coulomb and exchange series in direct space is controlled by setting the Gaussian overlap tolerance criteria to 10^{-7}, 10^{-7}, 10^{-7}, 10^{-7}, and 10^{-14}. A linear mixing of 70% and Anderson second-order mixing scheme are applied in the self-consistent field (SCF) iterations to accelerate convergence. Mulliken population analysis is used to estimate atomic contributions to the total charge and spin density. Unconstrained converged SCF solutions are obtained for different electronic spin configurations by controlling the spin density of the initial density matrix.

The computed ground-state electronic structure, displayed in Fig. 2, and density of states plots (Fig. 3) show the half-metallic character. The majority-spin electrons occupy bands that cross the Fermi level, E_F, where the corresponding density of states is gapless. Conversely, a band gap of 1.79 eV is present in the minority-spin bands and related density of states. The nature of the majority-spin electronic structure is therefore metallic while the system is an insulator for the minority-spin electrons. Detailed analysis of the states contributing to the electronic structure shows that the metallic character for the majority-spin electrons is mostly confined to the flat Nb-$[TCNE]_{eq}$ planes. The broad majority-spin bands crossing the Fermi energy in the region of the F point (shown as dashed-dotted lines in Fig. 2) are due to strong hybridization between the Nb d_{xz} and d_{yz} orbitals and the

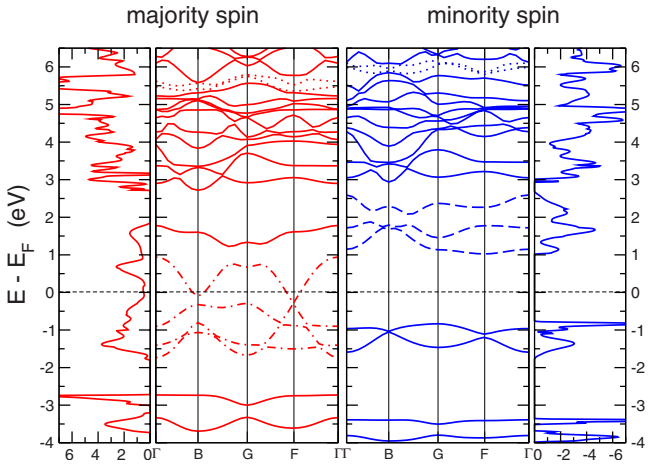

FIG. 2. (Color online) The electronic structure of $Nb(TCNE)_2$ in its ground-state ferrimagnetic configuration. From left to right the four panels represent: the density of states and the electronic band structure of the majority-spin electrons (in red online); the electronic band structure and the density of states of the minority-spin electrons (in blue online). The dashed-dotted, dashed, and dotted lines correspond, respectively, to the hybridized Nb t_{2g}-TCNEπ^*, Nb t_{2g}, and e_g states. The energy scale (electron volt) is expressed relatively to the Fermi energy, E_F.

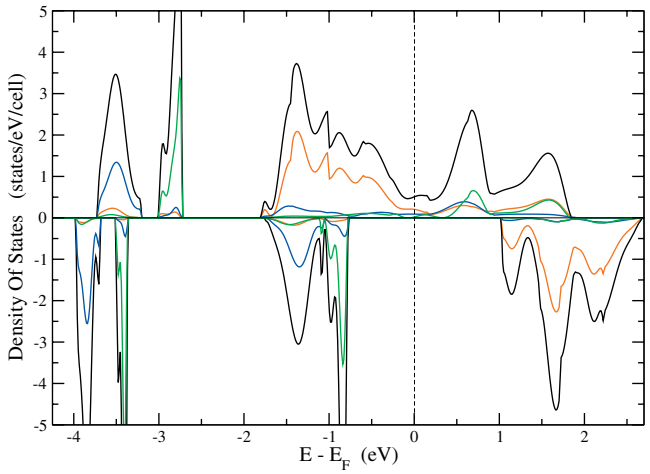

FIG. 3. (Color) Total (black line) and partial density of states of the ground state. The orange line represents the contribution of the Nb d states, the green line the equatorial TCNE p states, and the blue line the apical TCNE p states. Positive and negative values denote majority and minority spins, respectively. The energy scale (in electron volt) is expressed relatively to the Fermi energy, E_F.

$[TCNE]^{\cdot-}$ π^* orbitals of the equatorial ligands. The band gap in the minority-spin states lies between $[TCNE]^{\cdot-}$ π^* states and unoccupied Nb t_{2g} states (dashed lines). This electronic structure is the result of a combination of on-site electron correlation and strong metal-ligand hybridization. The Nb d states are separated into t_{2g}-like and e_g-like subbands (the latter depicted as dotted lines in Fig. 2) by a crystal-field splitting of approximately 4.3 eV.

In Ref. 4 we reported results from first-principles calculations for the compound $V(TCNE)_2$ which is known to be a semiconducting ferrimagnet. It is interesting to explore why $V(TCNE)_2$ is semiconducting whereas $Nb(TCNE)_2$ is half-metallic. Both Nb and V belong to group 5 of the periodic table, with V belonging to period 4, and Nb to period 5. As a result of the more diffuse nature of the Nb 4d with respect to the V 3d orbitals, the substitution of V with Nb in $M(TCNE)_2$ compounds induces a significantly enhanced metal-ligand interaction. The calculations indicate the formation of metallic hybridized Nb/TCNE bands which evidences an enhanced π backbonding interaction due to a considerable overlap between the metal 4d and the equatorial TCNE 2p orbitals.

The electronic band structure can be interpreted in terms of the Hamiltonian first introduced by Hubbard,[23]

$$\hat{H}^{Hubbard} = -t\sum_{\langle i,j\rangle}\sum_{\sigma}(c^{\dagger}_{i\sigma}c_{j\sigma} + c^{\dagger}_{j\sigma}c_{i\sigma}) + U\sum_{i}\hat{n}_{i\uparrow}\hat{n}_{i\downarrow}, \quad (1)$$

where t is the nearest-neighbor transfer integral, U is the on-site Coulomb repulsion and $c^{\dagger}_{i\sigma}$ and $c_{i\sigma}$ are the creation and annihilation operators of an electron with spin $\sigma=\uparrow,\downarrow$ at site i, with i being a lattice site index. Here $\hat{n}_{i\sigma}$ represents the occupation number operator which is defined as $\hat{n}_{i\sigma}=c^{\dagger}_{i\sigma}c_{i\sigma}$. By fitting this Hamiltonian to the calculated band structure we obtain a Hubbard parameter $U\approx 3$ eV for the Nb t_{2g} states. As the bandwidth of these states is of order 0.3 eV (see Fig. 2), this corresponds to a strong on-site electron correlation regime, leading to the formation of a t_{2g} lower Hubbard band of majority-spin states and a t_{2g} upper Hubbard band of minority-spin states. The d_{xz} and d_{yz} electrons of the lower Hubbard band hybridize strongly with the π^* orbitals of the equatorial ligand with an effective hopping parameter $t_{d-\pi^*}$ of approximately 1 eV to produce the delocalized metallic states of the 2D sheet. The in-plane d_{xy} states interact relatively weakly with the equatorial and apical ligands and form a narrow band of localized states at around −1.20 eV.

In order to assess the influence of the approximate treatment of electronic exchange and correlation on the half-metallic character, the ground-state calculation was repeated using a generalized gradient-corrected approximation [PBE (Ref. 24)] and an alternative hybrid-exchange functional [PBE0 (Ref. 25)]. It was found that the prediction of the half-metallic character is robust with respect to all exchange-correlation functionals tested here. Compared to B3LYP, PBE0 leads to increased electronic localization and a larger band gap in the minority-spin channel (2.34 eV) while PBE gives a much more diffuse electronic density, with a minority-spin gap of 0.18 eV.

The presence of unpaired electrons results in spin moments whose mutual interaction determines the macroscopic magnetic character of the material. The plot of the spin-density difference in Fig. 4 illustrates the areas of excess of majority- and minority-electron spin densities in the ground state. The spin density can be partitioned in the three chemical units that compose the crystal: the Nb ion and the equatorial and apical $[TCNE]^{\cdot-}$ radicals. In the ground state the spin moment on the Nb ion is aligned in an antiparallel fashion to both spin moments on the $[TCNE]^{\cdot-}$ molecules, resulting in ferrimagnetic order with a total magnetic moment of 1 μ_B per formula unit. The prediction of a ferrimagnetic ground state agrees with magnetization measurements in thin films which detected ferrimagnetic order up to 210 K, a saturation magnetization of 6×10^{-4} emu Oe g^{-1} and a coercive field of 200 Oe at 2 K.[15–17]

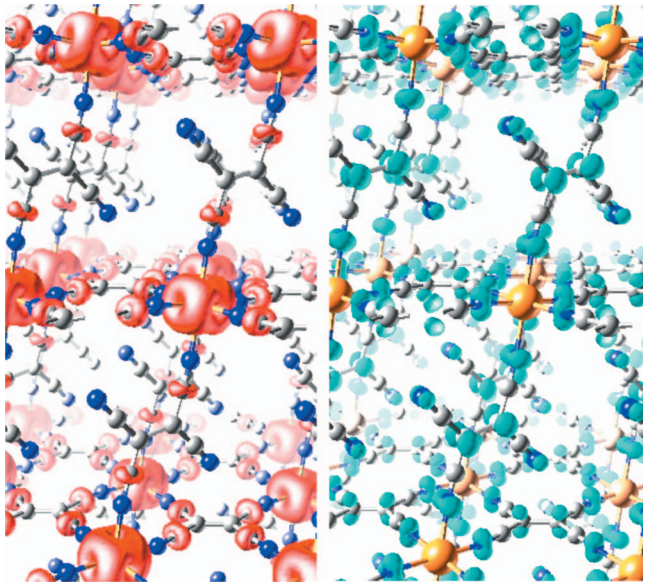

FIG. 4. (Color) Plot of the spin-density difference $(\rho_\uparrow-\rho_\downarrow)$ for the ferrimagnetic ground state. The left-hand panel shows the excess of majority-spin density (in red, isosurface value= +0.009 $e/\text{Å}^3$) while the right-hand panel shows the excess of minority-spin density (in blue, isosurface value=−0.011 $e/\text{Å}^3$). The distribution of the spin-density difference in the planes is visible most clearly at the bottom of the figures while the distribution of spin-density difference on the apical $[TCNE]^{\cdot-}$ ion is best shown toward the top.

The local exchange repulsion ensures that in the ground state the unpaired electrons on each atom are coupled in an antiparallel fashion to those on its nearest neighbor (the vinyl C atoms act a single spin unit in this respect because they share a double bond). This spin alternation mechanism generates long-range magnetic coupling which has been observed previously in π-bonded organic networks.[26] Any other state that violates this alternation will do so at an energy cost. An estimate of the energy scale for spin fluctuations and, hence, for the thermal stability of the ground state is given by the energy difference with the next lowest energy state. The energies and total magnetic moment per unit cell and the Mulliken spin populations of Nb ion, equatorial $[TCNE]^{\cdot-}$ and apical $[TCNE]^{\cdot-}$ for the ground state and next lowest energy state are shown in Table I. In the lowest en-

TABLE I. Total magnetic moment (S) per unit cell, Mulliken spin population (μ) of Nb, equatorial and apical TCNE, and total-energy differences (ΔE_{tot}) with respect to the ground state ($S=1$ μ_B p.u.c.) for the computed spin configurations.

Configuration	S (μ_B p.u.c.)	Spin unit	$\mu[\lvert e\rvert]$	ΔE_{tot} (eV p.u.c.)
FI	+1	Nb	+1.77	
		$[TCNE]^-_{eq}$	−0.12	
		$[TCNE]^-_{ap}$	−0.65	
FO	+2.74	Nb	+1.59	+0.217
		$[TCNE]^-_{eq}$	+0.22	
		$[TCNE]^-_{ap}$	+0.90	

ergy state found that breaks this spin alternation rule the net spin moments on the Nb ion and $[TCNE]^{\cdot-}$ radicals are all parallel to each other, giving ferromagnetic order with a total spin moment of 2.74 μ_B per formula unit. The analysis of the spin-density maps indicates that the spin alternation mechanism is violated in the direction perpendicular to the Nb-$[TCNE]_{eq}$ planes, at a significant energy cost (of ~0.2 eV per unit cell). In the Nb-$[TCNE]_{eq}$ planes the spin alternation is still fully respected and the change in the sign of the $[TCNE]_{eq}$ net spin moment is due to a variation in the size of the local atomic moments rather than to a change in their sign. A stable state where the spin alternation rule is violated in the planes could not be found. The reluctance of the system to break the spin alternation pattern in the planes is further evidence of the strong itinerant magnetism present in the planes, where the Nb-$[TCNE]_{eq}$ hybridized electronic states reside giving rise to the half-metallic character of the material. It is therefore the magnetic interactions along the chains that determines the magnetic ordering temperature while the electronic interactions in the planes determine the half-metallic character of the material. Each layer in this system therefore supports a quasi-two-dimensional metal. Further experimental and theoretical studies of this property, and its interaction with applied magnetic fields, would be of great interest.

In conclusion, the metal-organic compound $Nb(TCNE)_2$ has been studied by means of electronic-structure calculations based on hybrid density-functional theory. The combination of strong on-site electron correlation between the Nb^{2+} d states and strong off-site hybridization with the equatorial $[TCNE]^{\cdot-}$ ligands produces a half-metallic state in which spin-polarized Nb^{2+}-$[TCNE]^{\cdot-}$ planes are separated by $[TCNE]_{ap}$ with strong ferrimagnetic order. In agreement with experiment, the compound is found to be a ferrimagnet with a high ordering temperature for this class of materials. In addition and most interestingly, $Nb(TCNE)_2$ is predicted to be a half-metal. A subtle combination of strong on-site electron correlation among the Nb^{2+} d states and strong off-site hybridization with the equatorial $[TCNE]^{\cdot-}$ ligands produces a half-metallic state in which spin-polarized Nb^{2+}-$[TCNE]^{\cdot-}$ planes are separated by $[TCNE]_{ap}$ with strong ferrimagnetic order. The prediction of the coexistence of these properties in $Nb(TCNE)_2$ may expand the fundamental interest in metal-organic compounds as promising materials for half-metallic and organic spintronics.

We thank the STFC for strategic initiative grant and the EPSRC for provision of computer time under the Materials Chemistry Consortium Project, Grant No. GR/S13422/01.

*Corresponding author; barbara.montanari@stfc.ac.uk

[1] J. M. Manriquez, G. T. Yee, R. S. McLean, A. J. Epstein, and J. S. Miller, Science **252**, 1415 (1991).
[2] J. S. Miller and A. J. Epstein, Chem. Commun. (Cambridge) 1319 (1998).
[3] K. I. Pokhodnya, D. Pejakovic, A. J. Epstein, and J. S. Miller, Phys. Rev. B **63**, 174408 (2001).
[4] G. C. De Fusco, L. Pisani, B. Montanari, and N. M. Harrison, Phys. Rev. B **79**, 085201 (2009).
[5] C. Felser, G. H. Fecher, and B. Balke, Angew. Chem., Int. Ed. Engl. **46**, 668 (2007).
[6] S. Pramanik, C.-G. Stefanita, S. Patibandla, S. Bandyopadhyay, K. Garre, N. Harth, and M. Cahay, Nat. Nanotechnol. **2**, 216 (2007).
[7] S. Sanvito and A. R. Rocha, J. Comput. Theor. Nanosci. **3**, 624 (2006).
[8] V. A. Dediu, L. E. Hueso, I. Bergenti, and C. Taliani, Nature Mater. **8**, 707 (2009).
[9] C. Taliani, V. A. Dediu, F. Biscarini, M. Cavallini, M. Murgia, G. Ruani, and P. Nozar, Phase Transitions **75**, 1049 (2002).
[10] Z. H. Xiong, D. Wu, Z. V. Vardeny, and J. Shi, Nature (London) **427**, 821 (2004).
[11] T. Furubayashi, K. Kodama, H. Sukegawa, Y. K. Takahashi, K. Inomata, and K. Hono, Appl. Phys. Lett. **93**, 122507 (2008).
[12] S. S. Mallajosyula and S. K. Pati, J. Phys. Chem. B **111**, 13877 (2007).
[13] Y.-W. Son, M. L. Cohen, and S. G. Louie, Nature (London) **444**, 347 (2006).
[14] S. Dutta, A. K. Manna, and S. K. Pati, Phys. Rev. Lett. **102**, 096601 (2009).
[15] D. de Caro, M. Basso-Bert, H. Casellas, M. Elgaddari, I.-P. Savy, J.-F. Lamère, A. Bachelier, C. Faulmann, I. Malfant, and L. Valade, C. R. Chim. **8**, 1156 (2005).
[16] D. de Caro, C. Faulmann, and L. Valade, Chem.-Eur. J. **13**, 1650 (2007).
[17] E. Lamouroux, E. Alric, H. Casellas, L. Valade, D. de Caro, M. Etienne, and D. Gatteschi, Electrochem. Soc. Proc. **8**, 1040 (2003).
[18] M. P. de Jong, C. Tengstedt, A. Kanciurzewska, E. Carlegrim, W. R. Salaneck, and M. Fahlman, Phys. Rev. B **75**, 064407 (2007).
[19] A. D. Becke, Phys. Rev. A **38**, 3098 (1988).
[20] A. D. Becke, J. Chem. Phys. **98**, 5648 (1993).
[21] C. Lee, W. Yang, and R. G. Parr, Phys. Rev. B **37**, 785 (1988).
[22] R. Dovesi *et al.*, CRYSTAL06 User's Manual, Università di Torino, Torino (2006).
[23] J. Hubbard, Proc. R. Soc. London **A276**, 238 (1963); **A277**, 237 (1964); **A281**, 401 (1964).
[24] J. P. Perdew, K. Burke, and M. Ernzerhof, Phys. Rev. Lett. **77**, 3865 (1996).
[25] C. Adamo and V. Barone, J. Chem. Phys. **110**, 6158 (1999).
[26] L. Pisani, B. Montanari, and N. M. Harrison, New J. Phys. **10**, 033002 (2008).